HHS Public Access

Author manuscript

Prog Neuropsychopharmacol Biol Psychiatry. Author manuscript; available in PMC 2019 December 20.

Published in final edited form as:

Prog Neuropsychopharmacol Biol Psychiatry. 2019 December 20; 95: 109684. doi:10.1016/j.pnpbp.2019.109684.

MG53 attenuates lipopolysaccharide-induced neurotoxicity and neuroinflammation *via* inhibiting TLR4/NF-κB pathway *in vitro* and *in vivo*

Fangxia Guan[a,b,1], **Xinkui Zhou**[a,1], **Peng Li**[a,c,1], **Yaping Wang**[a], **Ming Liu**[a], **Fangfang Li**[a], **Yuanbo Cui**[a], **Tuanjie Huang**[a], **Minghao Yao**[a], **Yanting Zhang**[a], **Jianjie Ma**[d,**], **Shanshan Ma**[a,*]

[a]School of Life Sciences, Zhengzhou University, Zhengzhou 450001, Henan, China

[b]Henan Provincial People's Hospital, Zhengzhou 450003, Henan, China

[c]Clinical Laboratory, Zhumadian Hospital of Traditional Chinese Medicine, Zhumadian 463000, Henan, China

[d]Department of Surgery, Davis Heart and Lung Research Institute, The Ohio State University, Columbus, OH 43210, USA

Abstract

Neuroinflammation plays important roles in the pathogenesis and development of neurodegenerative disorders. Lipopolysaccharide (LPS) induces neuroinflammation and causes neurotoxicity, which results in cell damage or memory impairment in different cells and animals. In the present study, we investigated the neuroprotective effects of MG53, a member of the TRIM family proteins, against LPS-induced neuroinflammation and neurotoxicity *in vitro* and *in vivo*. MG53 significantly protected HT22 cells against LPS-induced cell apoptosis and cell cycle arrest by inhibiting TNF-α, IL-6 and IL-1β expression. In addition, MG53 ameliorated LPS-induced memory impairment and neuronal cell death in mice. Interestingly, MG53 significantly promoted newborn cell survival, improved neurogenesis, and mitigated neuroinflammation evidenced by lower production of IL-1β and IL-6, less activation of microglia in the hippocampus of LPS treated mice. Further studies demonstrated that MG53 significantly inhibited TLR4 expression and nuclear factor-κB (NF-κB) phosphorylation in LPS treated HT22 cells and mice. Taken together,

*Correspondence to: S. Ma, School of Life Sciences, Zhengzhou University, No.100 Science Avenue, Zhengzhou 450001, Henan, China. mss@zzu.edu.cn (S. Ma). **Correspondence to: J. Ma, Department of Surgery, Davis Heart and Lung Research Institute, The Ohio State University, Columbus, OH 43210, USA. Jianjie.Ma@osumc.edu (J. Ma).

[1]These authors contributed equally to this work.

Author contributions

SSM and FXG conceived and designed the experiments, JJM, SSM and FXG revised the final version of the paper. XKZ and PL performed the experiments. YPW, ML and FFL made the behavior test. XKZ and PL analyzed the data. SSM, PL, YBC and FXG wrote the manuscript, YPW, ML, FFL, TJH, MHY and YTZ prepared reagents and materials and performed part of the experiments. All authors reviewed the manuscript prior to submission.

Ethical statement

This study was approved by the Ethics Committees of the Zhengzhou University. The animal procedures were conducted in strict accordance with the National Institutes of Health guidelines for the Care and Use of Laboratory Animals.

Declaration of Competing Interest

The authors declare that they have no conflict of interest.

our results suggested that MG53 attenuated LPS-induced neurotoxicity and neuroinflammation partly by inhibitingTLR4/NF-κB pathway *in vitro* and *in vivo*.

Keywords

MG53 protein; Lipopolysaccharide; Neurotoxicity; Cognitive impairment; TLR4/NF-κB pathway

1. Introduction

Neuroinflammation plays an important role in the pathogenesis and progression of some neurodegenerative diseases such as Alzheimer's disease (AD) (Sawikr et al., 2017). AD is characterized by obvious cognitive impairment and neuroinflammation, including activation of glial cells and increased production of pro-inflammatory cytokines (Lane et al., 2018). Meanwhile, neuroinflammation is regarded as a key factor in the secondary injury cascade and contributes to neuronal death and neurological deterioration (Russo and McGavern, 2016). Hence, it is necessary to find novel anti-inflammatory agents to prevent the progression of AD through modulation of neuroinflammation.

Neurotoxicity could induce neuronal death and dysfunction of the neural network in neural cells (Mouton et al., 2012). Lipopolysaccharides (LPS), a component of gram-negative bacteria, is widely used to activate inflammation (Lee and Jeong, 2014; Musa et al., 2017; Prince et al., 2017). Previous studies have shown that LPS could result in cell death *in vitro* and administration of LPS could cause cognitive disorders *in vivo* by inducing neurotoxicity (Wu et al., 2019). In addition, LPS is a potent ligand of toll-like receptor 4 (TLR4), which stimulates the activation of nuclear factor kappa B (NF-κB) and the associated expression of proinflammatory mediators, such as tumor necrosis factor α (TNF-α) and interleukin-6 (IL-6) (Du et al., 2017; Gao et al., 2017a; Nyati et al., 2017). Numerous studies have shown that TLR4/NF-κB signaling pathway plays a key role in the pathogenesis of neuroinflammation (Du et al., 2017; Nyati et al., 2017; Yuan et al., 2013; Ha et al., 2014; Shirjang et al., 2017).

MG53, a member of the tripartite motif (TRIM) family protein, is also an essential component of the cell membrane repair machinery (Cai et al., 2009a; Weisleder et al., 2012). MG53 is predominantly expressed in skeletal and cardiac muscles, lung and kidney (Weisleder et al., 2012; Jia et al., 2014; Duann et al., 2015). The recombinant human MG53 (rhMG53) protein can protect various cell types against membrane disruption, such as cardiac muscles, epithelial, neuronal, and immune origin cells (Weisleder et al., 2012). In addition, exogenous rhMG53 has protective effects in treatment or prevention of muscular dystrophy(Weisleder et al., 2012), lung injury(Jia et al., 2014), and acute kidney injury(Duann et al., 2015) in many animal models. Furthermore, there is no MG53 expression in the mouse brain and neuronal cells(Yao et al., 2016). But, rhMG53 could prevent cultured neuronal cells from injuries *in vitro*, and MG53 could permeate through blood-brain barrier to protect acute brain injury *in vivo* (Yao et al., 2016). However, the protective effects of MG53 on LPS-induced neurotoxicity in neuronal cells and animal models remain unknown.

In the present study, we investigated whether MG53 could protect HT22 cells and C57BL/6 mice against LPS-induced neurotoxicity, and then further explored the anti-inflammatory roles of TLR4/NF-κB pathway mediated by MG53. Our results may provide new insights into the neuroprotective effect of MG53 and the potential novel anti-inflammatory strategy induced by LPS.

2. Materials and methods

2.1. Materials

LPS, purified from *Escherichia coli* O111:B4, was purchased from Sigma-Aldrich (St.Louis, MO, U.S.A.) and was dissolved in 1% ethanol to experiments. Purification of recombinant human MG53 protein has been described previously (Yao et al., 2016). MG53 was lyophilized and stored at 4 °C. For intravenous injection of rhMG53, the protein was diluted in 0.9% sterile saline, filtered through a 0.22-μm filter, and injected *via* the tail vein.

2.2. Culture of HT22 and cell viability analysis

HT22 cell is a mouse hippocampal neuronal cell line. In our study, HT22 cells were purchased from Guangzhou Jennio Biotech Co., Ltd. LPS (*E. coli*, serotype 055: B5). HT22 cells were maintained in high-glucose Dulbecco's Modified Eagle Medium (DMEM) containing 10% fetal bovine serum and 1% penicillin/streptomycin, and then cultured in a humidified 5% CO_2 incubator at 37 °C.

Briefly, HT22 cells were seeded in a 96-well plate at a density of 5×10^3 cells/well, then treated with different concentrations (25, 50, 100, 250, 500, 1000, 1500 μg/ml) of LPS at different intervals of 12, 24, 36, 48, and 60 hs. The cell viability was evaluated by using CCK-8 assay (Wang et al., 2016). Cell viability was confirmed by measuring the absorbance at 450 nm using a microplate reader (Thermo, USA). Then, HT22 cells in these experiments were divided into 4 groups: NC group (without LPS), MG53 group (treatment with 30 μg/ml MG53), LPS group (treatment with 500 μg/ml LPS), and MG53 + LPS group (pretreatment with 30 μg/ml MG53 for 8 h before 500 μg/ml LPS stimulation).

2.3. Flow cytometry analysis

HT22 cells were incubated with or without 30 μg/ml MG53 for 8 h and then 500 μg/ml LPS stimulation for 48 h. The procedures of cell cycle and cell apoptosis analysis were performed according to the manufacturer's instructions (BD Biosciences, USA) as previously described (Wang et al., 2016).

2.4. Determination of SOD and MDA in vitro

The activity of SOD and the concentration of MDA in HT22 cells of each group were determined using the commercial kit as previously reported (Xu et al., 2019). The procedures were following the users' manual.

2.5. Animal experiments

A total of 72 male C57BL/6 mice (8–12 w, 22–25 g) were obtained from Beijing Vital River Laboratory Animal Technology Co., Ltd. (China). All the experimental procedures were

accordance with the National Institutes of Health guidelines for the Care and Use of Laboratory Animals and approved by Animal Ethics Committee of Zhengzhou University.

The mice were randomly divided into 3 groups: Control (Con) group, LPS group, MG53 + LPS group. For the control group, mice were injected with the same volume of 0.9% saline. For the LPS group, LPS (0.25 mg/kg) was intraperitoneally injected once a day for 1 week to induce memory impairment and neuroinflammation. For the MG53 + LPS group, MG53 protein (2 mg/kg, once a day for 2 weeks) was intravenously administrated through tail vein one week prior to LPS injection. The timeline for animal experiments were showed in Fig. 4A. The following behavioral tests were performed by double-blind trials to the experiments.

2.6. Morris water maze (MWM)

The MWM test was used to analyze the learning and memory function of mice based on previously described (Wang et al., 2018). Each mouse underwent four trials a day for 6 days from day 15 to day 21. Probe trials and navigation tests were performed on day 21. The latency to find the hidden platform (escape time), number of crosses over the platform location, the time spent in the target quadrant (T%) and the speed were recorded by a video tracking system (Chengdu Taimeng Tech. Co. LTD, China).

2.7. Novel object recognition (NOR) test

On day 21, NOR test was also used to assess the learning and memory ability as previously described (Cheng et al., 2016). A discrimination index (total time spent with new object/total time devoted to exploration of objects) was calculated for each mouse.

2.8. Open field test (OFT)

The open-field test (OFT) was used to detect the locomotor activity and spatial exploration ability of mice as previously described (Heredia et al., 2014). The total ambulatory distance traveled in the maze and the number of rearings were calculated within 3 min.

2.9. Tissue preparation

Mice were anesthetized and perfused intracardially with ice-cold 0.9% saline. Then, the mice were sacrificed and the brain tissues were collected. The brain tissues were incubated in ice-cold 4% paraformaldehyde (PFA) at 4 °C overnight, then transferred into 30% sucrose solution and incubated for 72 h. Afterwards, the brain tissues were cut on a cryostat (Leica, Germany) to obtain 10 μm frozen serial coronal sections and the sections were stored at −80 °C until further processing.

2.10. EdU/NeuN-labeling assays

Mice were given 5 mg/kg EdU by intraperitoneal Injections 48 h before sacrifice. Brains were fixed in 4% PFA and embedded. Proliferation was evaluated by Cell-LightTM Edu Apollo Kit (RiboBio Co., Ltd., China) according to the manufacturer's protocol. After Apollo staining, washed sections were incubated with a rat antibody against NeuN (1:200, Proteintech, China) at 4 °C overnight and incubated with FITC conjugated goat anti-rabbit IgG (1:500, Proteintech, China) for 1 h at room temperature, followed by DAPI (1:2000,

Biotech, China) staining for 10 min. Then, stained sections were examined with a microscope (Eclipse TE2000-E; Nikon). The average number of EdU/NeuN-positive cells was analyzed by Image J software (NIH, Bethesda, MD, USA) and divided by the total area in the image field (mm^2).

2.11. TUNEL staining

TUNEL staining was performed to assess the cell apoptosis in the brain by using *In Situ* Cell Death Detection Kit (Solarbio, China) according to manufacturer's protocol. Before antigen retrieval, frozen coronal brain sections were incubated with proteinase K for 10 min and washed three times with PBS. Then, sections were incubated with TdT enzyme containing FITC-labeled dUTP at 37 °C for 60 min. After washing with PBS, sections were stained with DAPI for 10 min, and TUNEL-positive cells were observed and counted under a fluorescence microscope (Eclipse TE2000-E; Nikon, Japan).

2.12. Nissl staining

After behavioral test, Nissl staining was used to evaluate the effect of MG53 on LPS-induced neuronal degeneration. The experiment of Nissl staining was performed as previously described (Cui et al., 2017).

2.13. Immunofluorescence staining

Immunofluorescence staining was used to detect the neurogenesis and neuroinflammation based on the previous description (Yuan et al., 2013; Wang et al., 2018). Briefly, after blocked, coronal sections were incubated with primary antibody of NeuN (1:200, Proteintech, China) and Iba-1 (1:200, Proteintech, China) at 4 °C overnight and then incubated with FITC -conjugated anti-mouse/rabbit IgG (1:500, Proteintech, China) for 1 h at room temperature, followed by DAPI (1:2000, Biotech, China) staining for 10 min. Stained sections were examined with a microscope (Eclipse TE2000-E; Nikon). The quantification of EdU, NeuN or Iba-1 positive cells was analyzed by Image J software (NIH, Bethesda, MD, USA) and divided by the total area in the image field (mm^2).

2.14. Western blot

The total proteins were extracted from HT22 cells and mice brain tissues in different groups. Equal amounts of protein were loaded and separated by SOS-PAGE and transferred to PVDF membrane (Millipore, USA) as previously described (Ma et al., 2014). The membrane was blocked in 5% skim milk and incubated with diluted primary antibodies: Cyclin Dl (1:500, Proteintech Group, Wuhan,China), Bcl-2 (1:200, Cell Signaling Technology, Danvers, MA, USA), Bax (1:200), TLR4 (1:500, CST), NF-κB (1:1000, CST), p-NF-κB (1:1000, CST), Iκβα (1:1000, CST), p –Iκβα (1: 1000, CST), IL-1β (1:500, Santa Cmz Biotechnology, Dallas, USA), IL-6 (1:500, Santa Cruz), TNF-α(1:500, Santa Cruz), β-actin (1:2000, Santa Cruz). The intensity of the resulting protein bands was quantified with Image J software (NIH, Bethesda, MD, USA).

2.15. Enzyme-linked Immunosorbent assay (ELISA)

Upon anesthesia, the peripheral blood of anesthetized mice was harvested and the serum was stored at −80 °C until processing. The release of IL-1β and IL-6 protein was measured using ELISA kits (Tsz Biosciences, Boston, MA, USA) according to the manufacturer's instructions.

2.16. Statistical analysis

All statistical procedures were carried out using SPSS 19.0 software for Windows (SPSS Inc., Chicago, IL, USA). The data of *in vitro* experimental was analyzed using two-way analysis of variance (ANOVA). All other data were analyzed by one-way ANOVA was used to examine significance between different groups *in vivo*. All results are expressed as mean ± SEM. *Post hoc* analysis were performed using Tukey–Kramer test in order to compare multiple groups. $p < .05$ was considered statistically significant.

3. Results

3.1. MG53 inhibites LPS-induced neurotoxicity in HT22 cells

CCK-8 assay was used to determine cell proliferation of HT22 cells. Low concentrations (25, 50, 100 μg/ml) of LPS promoted cell proliferation, while LPS with high concentration (250 and 500 μg/ml) inhibiting cell growth in a time and dose-dependent manner ($p < .05$, Fig. 1A, B). In the presence of 1000 μg/ml LPS, most cells died at the first day after LPS treated ($p < .05$, Fig. 1B). It is worth noticing that 500 μg/ml LPS treatment for 48 h, the inhibition rate of cell proliferation was close to 50%. Therefore, 500 μg/ml LPS treated for 48 h was used in the following experiments. In addition, to assess the protective effect of MG53, the cultured cells were pretreated with 30 μg/ml MG53 for 8 h, and then exposed to 500 μg/ml LPS. Results showed that LPSinduced cell growth inhibition was significantly rescued by MG53, with the cell viability rate rise from 56.40 ± 4.0% to 78.49 ± 6.6% ($p < .05$, Fig. 1C).

3.2. MG53 reverses LPS-induced cell cycle arrest and cell apoptosis in HT22 cells

The effects of MG53 or/and LPS on the cell cycle were evaluated by using flow cytometry. As shown in Fig. 2A and B, there was a significant arrest in the percentage in G0/G1 phase and a concomitant decrease in S phase after LPS treatment ($p < .05$, Fig. 2A, B). Besides, the expression of cell cycle related protein Cyclin Dl was downregulated after LPS treatment ($p < .05$, Fig. 2E, F). However, MG53 effectively protected HT22 cells against LPS induced cell cycle arrest and increased the expression of Cyclin D1 ($p < .05$, Fig. 2). Furthermore, Annexin V/PI staining and western blot were used to analyze the apoptosis of HT22 cells. As shown in Fig. 2 C and D, LPS significantly induced apoptosis in HT22 cells compared with the NC group (66.06 ± 4.91% *vs.* 4.33 ± 1.71%, $p < .05$). In the presence of MG53 (30 μg/ml), the number of early apoptotic cells in HT22 was significantly decreased (32.00 ± 3.26% *vs.* 66.06 ± 4. 91%, $p < .05$). In addition, LPS markedly suppressed the protein expression of Bcl2 and promoted Bax expression (Fig. 2E, F, $p < .05$). But, the expression of Bcl2 was reversed by MG53 (Fig. 2 E, F, $p < .05$). These data indicated that MG53 could attenuate LPS-induced cell cycle arrest and cell apoptosis in HT22

3.3. MG53 suppresses pro-inflammatory factor expression and TLR4/NFκB signal activation in LPS treated HT22 cells

To determine whether MG53 is a regulator of LPS-triggered neuroinflammation, the expression of pro-inflammatory markers was evaluated by western blot. Compared with the NC group, LPS significantly increased the expressions of IL-1β, TNF-α and IL-6 ($p < .05$). However, these increases were significantly abrogated by MG53 ($p < .05$, Fig. 3A and B). Furthermore, western blot was also used to examine the protein expressions of TLR4/NF-κB signal pathway to explore the anti-inflammatory mechanism of MG53. As shown in Fig. 3C and D, the protein expression of TLR4, phosphorylated NF-κB (p-NF-κB) and phosphorylated IκBα (p-IκBα) were increased by LPS ($p < .05$). However, MG53 inhibited the LPS-induced TLR4, p-NF-κB and p-IκBα expression ($p < .05$). In addition, the total expression of NF-κB was not affected ($p < .05$). Total IkBα expression was significantly decreased after LPS treatment, but was rescued by MG53 ($p < .05$). These findings indicated that MG53 suppressed LPS-induced neuroinflammation by inhibiting TLR4/NF-κB signaling mediated pro-inflammatory factor expression in HT22 cells.

3.4. MG53 ameliorates LPS-induced memory impairment in C57BL/6 mice

To investigate the neuroprotective effects of MG53 on the LPS-induced memory impairment *in vivo*, MWM test was performed to evaluate the cognitive function of LPS treated mice. The experimental outline was summarized in Fig. 4A. Compared with the Con group, the LPS-treated C57BL/6 mice showed significant cognition deficit in the MWM test ($p < .05$, Fig. 4B). However, pretreatment with MG53 in LPS-induced mice showed shorter escape latency, higher proportion of time spent in the target quadrant and more platform crossing numbers compared with the LPS group ($p < .05$, Fig. 4B–E). However, there were no significant differences in the swimming velocity between different groups (Fig. 4F, $p > .05$). In addition, in the MG53 + LPS group, MG53 significantly increased the discrimination index in the novel object recognition (NOR) test, and promoted total number of rearings and total ambulatory distance in the open field test (OFT) compared with those in LPS group ($p < .05$, Fig. 4G–I). These results suggested that MG53 ameliorated LPS-induced memory and cognitive impairment in mice.

3.5. MG53 prevents LPS-induced neuronal apoptosis in the hippocampus of LPS-treated mice

The cell death in the brain was measured by TUNEL staining. As shown in Fig. 5, LPS significantly increased the number of TUNEL-positive cells compared with the Con group ($p < .05$). However, MG53 significantly decreased LPS-induced TUNEL-positive cells ($p < .05$, Fig. 5A, B), which was further confirmed by the up-regulated expression of Bcl-2 and down-regulated Bax expression in the hippocampus ($p < .05$, Fig. 5C, D). These results indicated that MG53 inhibited LPSinduced neuronal apoptosis in the hippocampus of LPS treated mice.

3.6. MG53 promotes neuronal survival and neurogenesis in hippocampus of LPS treated mice

Nissl staining was used to observe the surviving neurons in hippocampus. Compared with the clear and intact neurons in the Con group, LPS significantly deceased the number of Nissl bodies and the neurons exhibited sparse cell arrangement ($p < .05$, Fig. 6A, B). However, the number of neurons was significantly increased and the cell layer was densely arranged in hippocampus of MG53 + LPS treated mice ($p < .05$, Fig. 6A, B). In addition, EdU and NeuN double-staining was used to observe hippocampal neurogenesis. Results showed that the number of EdU+ /NeuN + cells in the hippocampus of MG53 and LPS co-treated mice was significantly increased compared with that in the LPS group ($p < .05$, Fig. 6C, D). These results suggested that MG53 pre-administration promoted neuronal survival and neurogenesis in hippocampus of LPS treated mice.

3.7. MG53 attenuates LPS-induced pro-inflammatory cytokine secretion by inhibiting TLR4/NF-κB signaling in the hippocampus of LPS treated mice

In order to examine the effect of MG53 on LPS induced neuroinflammation *in vivo*, Iba-1 staining was used to detect the activation of microglia. As shown in Fig. 7A and B, there was more Iba-1 positive cells (activated microglia) in the hippocampus of the LPS-treated mice ($p < .05$), whereas MG53 pre-treatment significantly decreased Iba-1 positive cells ($p < .05$). In addition, ELISA was used to examine the release of IL-1β and IL-6. The administration of LPS significantly promoted the release of IL-1β and IL-6 ($p < .05$). However, MG53 significantly reduced the levels of IL-1β and IL-6 ($p < .05$) induced by LPS (Fig. 7C, D). Furthermore, western blot was used to examine the expression of TLR4/NF-κB signaling pathway. Consistent with our in vitro studies, our finding showed that the protein expression of TLR4, p-IKBα and p-NF-κB was significantly increased in the hippocampus of LPS-treated mice, whereas MG53 significantly inhibited TLR4, p- IκBα and p-NF-κB expression compared with those in the LPS treated group ($p < .05$, Fig. 8E, F). These data indicated that MG53 attenuated LPSinduced neuroinflammation *in vivo*, and the mechanism was partly involved in the inhibition of TLR4/NF-κB signaling pathway.

4. Discussion

The integrity of plasma membrane plays an important role in maintaining the cellular homeostasis, and the defect of plasma membrane results in cell death and numerous disease, including neurodegeneration (Bansal and Campbell, 2004; McElhanon and Bhattacharya, 2018). Protective effects of MG53 on cell membrane repair and tissue damage have been reported in recent studies (Weisleder et al., 2012; Jia et al., 2014; Duann et al., 2015). In muscle membrane repair, MG53 binds to phosphatidylserine (PS) and interacts with caveolin-3 (Cav-3) to mediate vesicle accumulation at injury sites upon cell membrane damage (Cai et al., 2009a; Cai et al., 2009b; Weisleder et al., 2009) involved in patching the membrane. In tissue repair, MG53 interacts with p85 subunit of PI3K as well as CaV3 and subsequent activates the pro-survival RISK pathway (including Pl3K/Akt/GSK3β cascade and ERKl/2 pathway) to protect ischemic brain injury and myocardial damage (Yao et al., 2016; Cao et al., 2010; Zhang et al., 2011). LPS induces neuroinflammation through activation of pro-inflammatory mediators and neurodegeneration (Prince et al., 2017; Wu et

al., 2019; Cheng et al., 2018; Khan et al., 2018a). But, whether MG53 exerts beneficial effects against LPS-mediated neuroinflammation and neurotoxicity remains unknown. In this study, we found that MG53 attenuated LPS-induced neuroinflammation and neurotoxicity *via* inhibiting TLR4/NF-κB pathway *in vitro* and *in vivo* (Fig. 8).

HT22 cells is a kind of mouse hippocampal neuronal cells, which are widely used as an *in vitro* neuronal model related with cognitive deficits and neurotoxicity. Many studies have demonstrated the neuroprotective effects of different phytochemicals on cognitive deficits and neurotoxicity via using HT-22 cells (Sun et al., 2015; Koh et al., 2017). In the present study, we used HT22 cells as a neuronal cell model to examine the protective effects of MG53 protein on LPS activated neurotoxicity. Previous studies have shown that LPS induced neurotoxicity leads to neuronal cell apoptosis and pro-apoptotic protein Bax and anti-apoptotic protein Bcl-2 are involved in regulating apoptosis (Musa et al., 2017). We found that LPS inhibited the viability of HT22 in a dose and time-dependent manner, accompanied by cell cycle arrest and cell apoptosis. However, pretreatment with MG53 significantly protected HT22 cells against LPS-induced cell growth inhibition by inhibiting apoptosis. These results were coincident with previous studies, which identified that MG53 improved the ability of membrane repair in muscle or non-muscle cells (Weisleder et al., 2012).

Previous studies have shown that systemic administration of LPS triggers neurotoxicity and neuroinflammation in the brain, which induce cognitive deficits and neurodegeneration in mice (Musa et al., 2017; Wu et al., 2019; Khan et al., 2018a; Muccigrosso et al., 2016). Then, we conducted behavior tests using MG53 in LPS treated mice by using MWM, NOR and OFT, which are series of behavior tests to investigate the learning and memory ability of animals (Xu et al., 2019; Wang et al., 2018; Cheng et al., 2016). We observed that MG53 prevented cognitive deficits and protected against LPS-induced neurotoxicity in the hippocampus of mice, as indicated by shorter escape latency, higher proportion of time spent in the target quadrant and more platform crossing times.

Previous studies reported that neuronal loss in the hippocampus is closely correlated with cognitive dysfunction (Russo and McGavem, 2016; Johnson et al., 2015; Jassam et al., 2017; Ngwenya and Danzer, 2018). Therefore, we determined neuronal cell death by using TUNEL staining. Our results indicated that MG53 significantly decreased LPSinduced neuronal cell death and Bax expression and promoted Bcl-2 expression in the hippocampus, which consistent with previous reports (Xu et al., 2019). On the other hand, nerurogenesis (Ngwenya and Danzer, 2018; de Miranda et al., 2017; Ramon-Canellas et al., 2019) is a multi-step process of the formation of new neurons in the hippocampus, and the newly generated neurons play a crucial role in learning and memory function and recovery from neuronal injury (Ngwenya and Danzer, 2018; de Miranda et al., 2017; Ramon-Canellas et al., 2019). In this study, results of Nissl staining and EdU/NeuN labeling revealed that LPS induced neuronal loss, while, the number of survival neurons and newborn cells were increased in the hippocampus of MG53 + LPS mice. Interestingly, significant increased number of Ki67 + /NeuN + cells was observed in the hippocampus of MG53 + LPS group compared with that in LPS group. These data indicated that MG53 promoted neurogenesis in hippocampus of LPS treated mice.

Chronic neuroinflammation mediates the neuronal apoptosis and degeneration process in various diseases, including Alzheimer's disease (AD). Both *in vivo* and *in vitro* studies, LPS activated cytokines release (Barcia et al., 2011) (such as IL-6, IL-1β and TNF-a) and microglia cells, which further trigger apoptotic neurodegeneration (Musa et al., 2017; Wu et al., 2019). In our study, Iba-1 was used to characterize the activation of microglia. Results showed that LPS seemed to activate the Iba-1 labeled microglia that caused the elevated levels of IL-1β and IL-6 in the hippocampus. While, MG53 pre-treatment significantly attenuated LPS induced neuroinflammation by decreasing Iba-1 positive cells and reversing the release of IL-1β and IL-6 in LPS treated mice and HT22 cells.

It has been known that TLR4/NF-κB signal plays critical roles in inflammatory cytokines release (Nyati et al., 2017; Ha et al., 2014; Shih et al., 2015). Toll-like receptors (TLR) signals promote rapid pro-inflammatory responses during bacterial infections (Vu et al., 2017) and initiate the inflammatory cascade (Du et al., 2017; Gao et al., 2017a; Nyati et al., 2017; Shirjang et al., 2017; Lim and Staudt, 2013; Gao et al., 2017b). TLR4 is a receptor of LPS and upregulated in neural and immune cells following LPS treatment (Mouton et al., 2012; Backhed et al., 2003; Choi, 2019). In normal conditions, the NF-κB protein is inactivated and bounds to IkBα in the cytoplasm (Zhao et al., 2014). When inflammatory reaction occurs, NF-κB is activated and promotes the production of inflammatory factors, such as TNF-α and IL-6 in the nucleus (Nyati et al., 2017; Li et al., 2015; Khan et al., 2018b). Our results demonstrated that LPS significantly activated the expressions of TLR4, p-NF-κB, TNF-α, IL-6 and IL-lβ in HT22 cells and experimental mice. While, these increases were significantly reversed by MG53 pre-administration *in vitro* and *in vivo*. But, rigorous TLR4 blocking evidence should be made in the future studies.

5. Conclusions

We demonstrated that MG53 treatment significantly attenuated LPS-induced neurotoxicity and neuroinflammation by partly inhibiting TLR4/NF-κB pathway *in vitro* and *in vivo*. Our results highlight the neuroprotective and anti-inflammatory effect of MG53, which suggests MG53 may act as a beneficial therapeutic agent in LPS-induced damage.

Acknowledgments

We thank all the members of the Dr. Fangxia Guan's laboratory for their discussion and suggestions on the project.

Funding

This study was supported by the National Natural Science Foundation of China (81601078), Science and Technology Research Project form Henan Province (152102310272), the Key Research Project of Higher Education of Henan Province (17A310012). US National Institutes of Health (R01-AR061385, R01-DK106394 and R01-AR070752).

References

Backhed F, Nonnark S, Schweda EK, Oscarson S, Richter-Dahlfors A, 2003 Structural requirements for TLR4-mediated LPS signalling: a biological role for LPS modifications. Microbes Infect 5, 1057–1063. [PubMed: 14554246]

Bansal D, campbell KP, 2004 Dysferlin and the plasma membrane repair in muscular dystrophy. Trends Cell Biol 14, 206–213. [PubMed: 15066638]

Barcia C, Ros CM, Annese V, Gomez A, Ros-Bernal F, Aguado-Llera D, MartinezPagan ME, de Pablos V, Fernandez-Villalba E, Herrero MT, signaling, IFNgamma, 2012 With the synergistic contribution of TNF-alpha, mediates cell specific microglial and astroglial activation in experimental models of Parkinson's disease. vol 2, el42, 2011. Cell Death Dis 3, e379. [PubMed: 22914327]

Cai CX, Masumiya H, Weisleder N, Matsuda N, Nishi M, Hwang M, Ko JK, Lin PH, Thornton A, Zhao XL, Pan Z, Komazaki S, Brotto M, Takeshima H, Ma JJ, 2009a MG53 nucleates assembly of cell membrane repair machinery. Nat. Cell Biol 11, 56–64. [PubMed: 19043407]

Cai C, Weisleder N, Ko JK, Komazaki S, Sunada Y, Nsihi M, Takeshima H, Ma J, 2009b Membrane repair defects in muscular dystrophy are linked to altered interaction between MG53, caveolin-3, and dysferlin. J. Biol. Chem 284 (23), 15894–15902. [PubMed: 19380584]

Cao CM, Zhang Y, Weisleder N, Ferrante C, Wang X, Lv F, Song R, Hwang M, Jin L, Guo J, Peng W, Li G, Nishi M, Takeshima H, Ma J, Xiao RP, 2010 MuS:J constitutes a primary determinant of cardiac ischemic preconditioning. Circulation 121, 2565–2574. [PubMed: 20516375]

Cheng T, Wang WZ, Li Q, Han XN, Xing J, Qi CF, Lan X, Wan JR, Potts A, Guan FX, Wang J, 2016 Cerebroprotection of flavanol (−)-epicatechni after traumatic brain injury via Nrf2-dependent and -independent pathways. Free Radie. Bio. Med 92, 15–28.

Cheng X, Yang YL, Yang H, Wang YH, Du GH, 2018 Kaempferol alleviates LPSinduced neuroinflamation and BBB dysfunction in mice via inhibiting HMGBl release and down-regulating TLR4/MyD88 pathway. Jnt. Immunophannacol 56, 29–35.

Choi YH, 2019 Catalpal attenuates lipopolysaccharide-induced inflammatory responses in BV2 microglia through inhibiting the TLR4-mediated NF-kappaB pathway. Gen. Physiol. Biophys 38 (2), 111–122. [PubMed: 30806632]

Cui Y, Ma S, Zhang C, Cao W, Liu M, Li D, Lv P, Xing Q, Qu R, Yao N, Yang B, Guan F, 2017 Human umbilical cord mesenchymal stem cells transplantation improves cognitive function in Alzhemimer's disease mice by decreasing oxidative stress and promoting hippocampal neurogenesis. Bebav. Brain Res 320, 291–301

de Miranda AS, Zhang CJ, Katsumoto A, Teixeira AL, 2017 Hippocampal adult neurogenesis: does the immune system matter? J. Neurol. Sci 372, 482–495. [PubMed: 27838002]

Du SH, Qiao DF, Chen CX, Chen S, Liu C, Lin ZM, Wang HJ, Xie WB, 2017 Toll-like receptor 4 mediates methamphetamine-induced neuroinflammation through caspase-11 si aling pathway in astrocytes. Front. Mol. Neurosci 10, 409. [PubMed: 29311802]

Duann P, Li H, Lni P, Tan T, Wang Z, Chen K, Zhou X, Gumpper K, Zhu H, Ludwig T, Mohler PJ, Rovin B, Abraham WT, Zeng C, Ma J, 2015 MG53-mediated cell membrane repair protects against acute kidney injury. Sci. Transl. Med 7, 279ra36.

Gao HW, Liu X, Sun W, Kang NX, Liu YL, Yang SL, Xu QM, Wang CM, Chen XP, 2017a Total tanshinones exhibits anti-inflammatory effects through blocking TLR4 dimerization via the MyD88 pathway. Cell Death Dis 8, e3004.

Gao W, Xiong Y, Li Q, Yang H, 2017b Inhibition of toll-like receptor si aling as a promising therapy for inflammatory diseases: a journey from molecular to nano therapeutics. Front. Physiol 8, 508. [PubMed: 28769820]

Ha VT, Beak HS, Kim E, Baek KS, Hassen MJ, Yang WS, Kim Y, Kim JH, Yang S, Kim JH, Joo YH, Lee CS, Choi J, Shni HJ, Hong S, Shin SS, Cho JY, 2014 NF-kappa B/AP-1-targeted inhibition of macrophage-mediated inflammatory responses by depigmenting compound AP736 derived from natural 1,3-Diphenylpropane skeleton. Mediat. Inflamm 2014, 354843 10.1155/2014/354843.

Heredia L, Torrente M, Colomina MT, Domingo JL, 2014 Assessing anxiety in C57BL/6J mice: a pharmacological characterization of the open-field and lighVdark tests. J. Phannacol. Tox. Methods 69, 108–114.

Jassam YN, Izzy S, Whalen M, McGavem DB, El Khoury J, 2017 Neuroimmunology of traumatic brain injury: time for a paradigm shift. Neuron 95 (6), 1246–1265. [PubMed: 28910616]

Jia Y, Chen K, Lin P, Lieber G, Nishi M, Yan R, Wang z., Yao Y, Li Y, Whitson BA, Duan P, Li H, Zhou X, Zhu H, Takeshima H, Hunter JC, McLeod RL, Weisleder N, Zeng C, Ma J, 2014 Treatment of acute lung injury by targeting MG53-mediated cell membrane repair. Nat. Commun 5, 4387. [PubMed: 25034454]

Johnson VE, Meaney DF, Cullen DK, Smith DH, 2015 Animal models of traumatic brain injury. Handb. Clin. Neural 127, 115–128.

Khan A, Ali T, Rebman SU, Khan MS, Alam S.l., lkram M, Muhammad T, Saeed K, Badshah H, Kim M0, 2018a Neuroprotective effect of quercetin against the detrimental effects of LPS in the adult mouse brain. Front. Phannacol 9, 1383.

Khan S, Wardill HR, Bowen JM, 2018b Role of toll-like receptor 4 (TLR4)-mediated interleukin-6 (IL-6) production in chemotherapy-induced mucositis. Cancer Chemoth. Phann 82, 31–37.

Koh EJ, Seo YJ, Choi J, Le HY, Kang DH, Kim KJ, Le BY, 2017 Spirulina maxima extract prevents neurotoxicity via promoting activation of signaling pathways in neuronal cells and mice. Molecules 22, 1363.

Lane CA, Hardy J, Schott JM, 2018 Alzheimer's disease. Eur. J. Neural 25 (1), 59–70.

Lee DS, Jeong GS, 2014 Arylbenzofuran isolated from Dalbergia odorifera suppresses lipopolysaccharide-induced mouse BV2 microglial cell activation, which protects mouse hippocampal HT22 cells death from neuroinflammation-mediated toxicity. Eur. J. Pharmacol 728, 1–8. [PubMed: 24485892]

Li Y, Zhao L, Fu H, Wu Y, Wang T, 2015 Ulinastatin suppresses lipopolysaccharide induced neuro-inflamation through the downregulation of nuclear factor-kappaB in SD rat hippocampal astrocyte. Biochem. Biophys. Res. Commun 458 (4), 763–770. [PubMed: 25681771]

Lim KH, Staudt LM, 2013 Toll-like receptor signaling. Cold Spring Harb. Perspect. Biol 5, a011247. [PubMed: 23284045]

Ma SS, Liang S, Jiao HL, Chi LK, Shi XY, Tian Y, Yang B, Guan FX, 2014 Human umbilical cord mesenchymal stem cells inhibit C6 glioma growth via secretion of dickkopf-1 (DKKl). Mol. Cell. Biochem 385, 277–286. [PubMed: 24104453]

McElhanon KE, Bhattacharya S, 2018 Altered membrane integrity in the progression of muscle diseases. Life Sci 192, 166–172. [PubMed: 29183798]

Mouton PR, Kelley-Bell B, Tweedie D, Spangler EL, Perez E, Carlson OD, Short RG, deCabo R, Chang J, Ingram DK, Li Y, Greig NH, 2012 The effects of age and lipopolysaccharide (LPS)-mediated peripheral inflammation on numbers of central catecholarninergic neurons. Neurobiol. Aging 33, 423 e27–36.

Muccigrosso MM, Ford J, Benner B, Moussa D, Burnsides C, Fenn AM, Popovich PG, Lifshitz J, Walker FR, Eiferman DS, Godbout JP, 2016 Cognitive deficits develop lmonth after diffuse brain injury and are exaggerated by microglia-associated reactivity to peripheral immune challenge. Brain Behav. Immun 54, 95–109. [PubMed: 26774527]

Musa NH, Mani V, Lim SM, Vidyadaran S, Abdul Majeed AB, Ramasamy K, 2017 Lactobaclili-fermented cow's milk attenuated lipopolysaccharide-induced neuroinflammation and memory impairment in vitro and in vivo. J. Dairy Res 84, 488–495. [PubMed: 29154736]

Ngwenya LB, Danzer SC, 2018 Impact of traumatic brain injury on neurogenesis. Front. Neurosci 12, 1014. [PubMed: 30686980]

Nyati KK, Masuda K, Zaman MM, Dubey PK, Mil D, Chalise JP, Higa M, Li S, Standley DM, Saito K, Hanieh H, Kishimoto T, 2017 TLR4-induced NFkappaB and MAPK signaling regulate the IL-6 mRNA stabli izing protein Arid5a. Nucleic Acids Res 45, 2687–2703. [PubMed: 28168301]

Prince PD, Fischerman L, Toblli JE, Fraga CG, Galleano M, 2017 LPS-induced renal inflammation is prevented by (–)-epicatechin in rats. Redox Biol 11, 342–349. [PubMed: 28039839]

Ramon-Canellas P, Peterson HP, Morante J, 2019 From early to late neurogenesis: neural progenitors and the glial niche from a Fly's point of view. Neuroscience 399, 39–52. [PubMed: 30578972]

Russo MV, McGavem DB, 2016 Inflammatory neuroprotection following traumatic brain injury. Science 353, 783–785. [PubMed: 27540166]

Sawikr Y, Yarla NS, Peluso I, Kamal MA, Aliev G, Bishayee A, 2017 Neuroinflammation in Alzheimer's disease: the preventive and therapeutic potential of polyphenolic nutraceuticals. Adv. Protein Chem. Struct. Biol 108, 33–57. [PubMed: 28427563]

Shih RH, Wang CY, Yang CM, 2015 NF-kappa B signaling pathways in neurological inflammation: a mini review. Front. Mol. Neurosci 8, 77. [PubMed: 26733801]

Shirjang S, Mansoori B, Solali S, Hagh MF, Shamsasenjan K, 2017 Toll-like receptors as a key regulator ofmesenchymal stem cell function: an up-to-date review. Cell. Immunol 315, 1–10. [PubMed: 28284487]

Sun J, Ren X, Simpkins JW, 2015 Sequential upregulation of superoxide dismutase 2 and hcrnc oxygcnasc 1 by tcrt-Butylhydroquinonc protects mitochondria during oxidative stress. Mol. Pharmacol 88, 437–449. [PubMed: 26082377]

Vu A, Calzadilla A, Gidfar S, Calderon-Candelario R, Mirsaeidi M, 2017 Toll-like receptors in mycobacterial infection. Eur. J. Pharmacol 808, 1–7. [PubMed: 27756604]

Wang XX, Ma SS, Meng N, Yao N, Zhang K, Li QH, Zhang YT, Xing Q, Han K, Song JS, Yang B, Guan FX, 2016 Resveratrol exerts dosage-dependent effects on the self-renewal and neural differentiation of hUC-MSCs. Mol. Cells 39, 418–425. [PubMed: 27109421]

Wang XX, Ma SS, Yang B, Huang TJ, Meng N, Xu L, Xing Q, Zhang YT, Zhang K, Li QH, Zhang T, Wu JW, Yang GL, Guan FX, Wang J, 2018 Resveratrol promotes hUC-MSCs engraftment and neural repair in a mouse model of Alzheimer's disease. Behav. Brain Res 339, 297–304. [PubMed: 29102593]

Weisleder N, Takeshirna H, Ma J, 2009 Mitsugumin 53 (MG53) facilitates vesicle trafficking in striated muscle to contribute to cell membrane repair. Commun. lntegr. Biol 2, 225–226.

Weisleder N, Takizawa N, Lin P, Wang X, Cao C, Zhang Y, Tan T, Ferrante C, Zhu H, Chen PJ, Yan R, Sterling M, Zhao X, Hwang M, Takeshima M, Cai C, Cheng H, Takeshima H, Xiao RP, Ma J, 2012 Recombinant MG53 protein modulates therapeutic cell membrane repair in treatment of muscular dystrophy. Sci. Transl. Med 4, 139ra85.

Wu X, Lv YG, Du YF, Hu M, Reed MN, Long Y, Suppiramaniam V, Hong H, Tang SS, 2019 Inhibitory effect of INT-777 on lipopolysaccharide-induced cognitive impairment, neuroinflammation, apoptosis, and synaptic dysfunction in mice. Prog. Neuro-Psychopharnnacol. Biol. Psychiatry 88, 360–374.

Xu L, Xing Q, Huang TJ, Zhou JK, Liu TF, Cui YB, Cheng T, Wang YP, Zhou XK, Yang B, Yang GL, Zhang JW, Zang XX, Ma SS, Guan FX, 2019 HDACl silence promotes neuroprotective effects of human umbilical cord-derived mesenchymal stem cells in a mouse model of traumatic brain injury via Pl3K/AKT pathway. Front. Cell. Neurosci 12, 489.

Yao Y, Zhang B, Zhu H, Li H, Han Y, Chen K, Wang Z, Zeng J, Liu Y, Wang X, Li Y, He D, Lin P, Zhou X, Park KH, Bian Z, Chen Z, Gong N, Tan T, Zhou J, Zhang M, Ma J, Zeng C, 2016 MG53 permeates through blood-brain barrier to protect ischernic brain injury. Oncotarget 7, 22474–22485. [PubMed: 26967557]

Yuan X, Zhou Y, Wang W, Li J, Xie G, Zhao Y, Xu D, Shen L, 2013 Activation of TLR4 signaling promotes gastric cancer progression by inducing mitochondrial ROS production. Cell Death Dis 4, e794. [PubMed: 24030146]

Zhang Y, Lv F, Jin L, Peng W, Song R, Ma J, Cao CM, Xiao RP, 2011 MG53 participates in ischaemic postconditioning through the RISK signalling pathway. Cardiovasc. Res 91, 108–115. [PubMed: 21285295]

Zhao M, Zhou A, Xu L, Zhang X, 2014 The role of TLR4-mediated PTEN/PI3K/AKT/NF-kappaB signaling pathway in neuroinflamation in hippocampal neurons. Neuroscience 269, 93–101. [PubMed: 24680857]

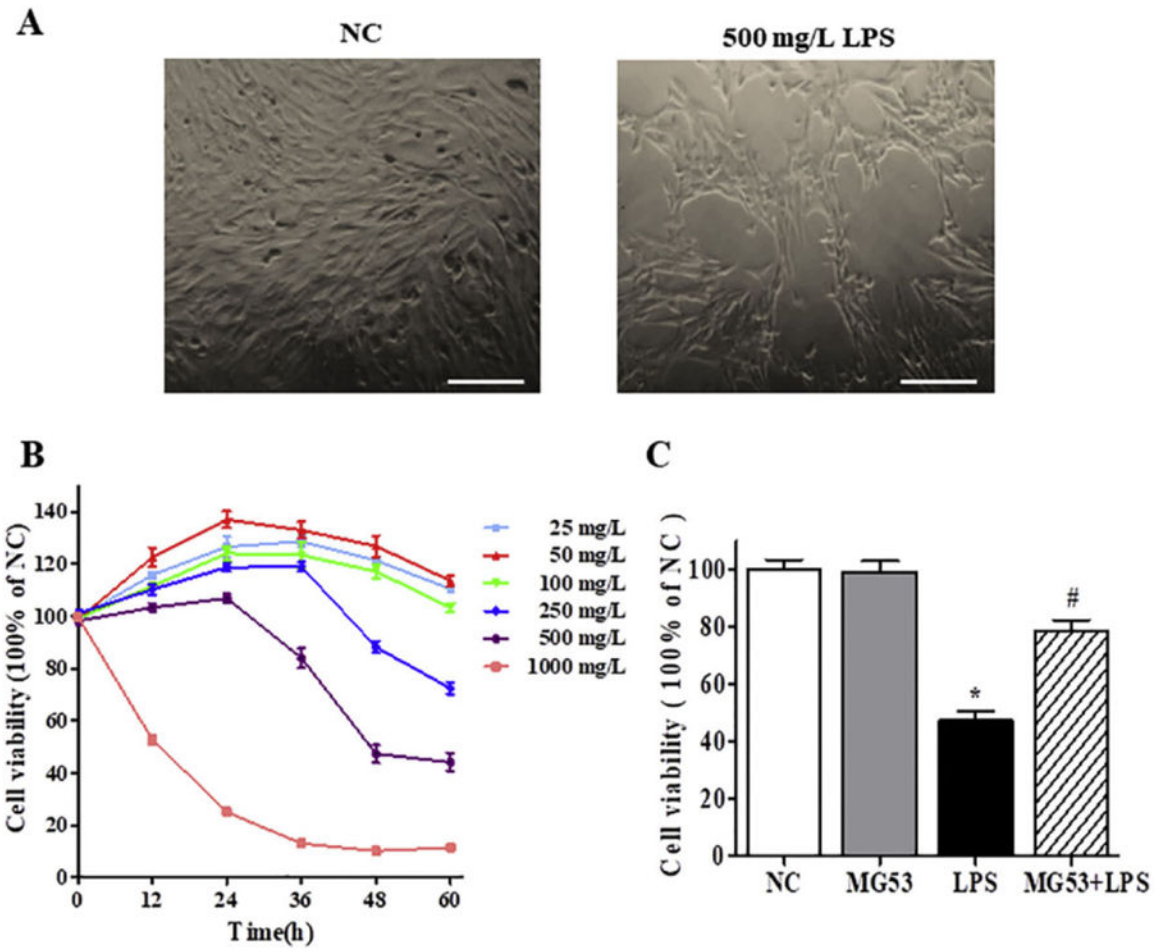

Fig. 1.

The effects of MG53 on cell viability of LPS-induced HT22 cells. (A) Representative images of HT22 with or without 500 μg/ml LPS for 48 h. Scale bar = 100 μm. (B) Effect of LPS on HT22 cells proliferation was measured by CCK-8 assay; (C) The effects of MG53 on cell viability of 500 μg/ml LPS-induced HT22. Data were presented as mean ± SEM. *$p < .05$ compared with NC group, $^{\#}p < .05$ compared with LPS group.

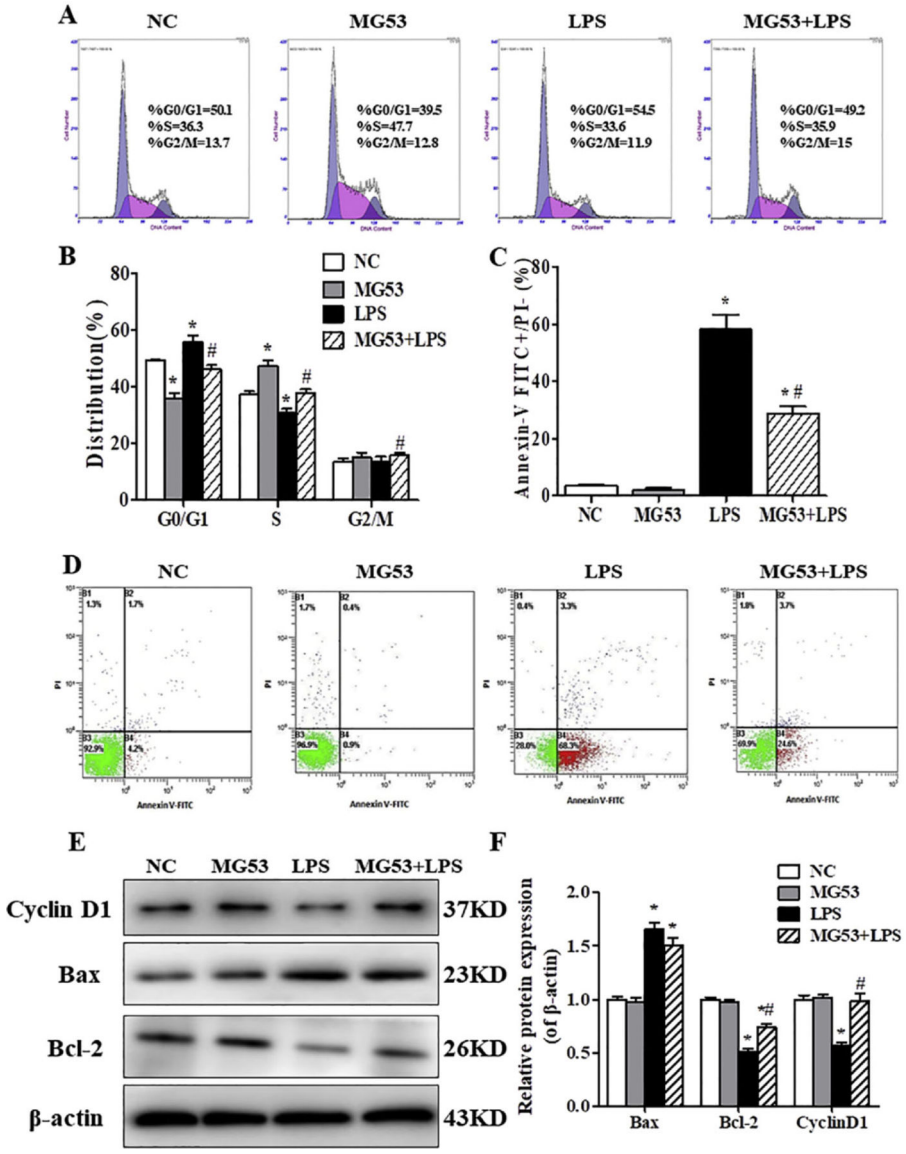

Fig. 2.

The effects of MG53 on cell cycle and cell apoptosis in LPS-induced HT22 cells. (A) Cell cycle was detected by flow cytometry. (B) Quantification of cell cycles. (C) Quantification of Annexin V/PI positive cells. (D) Apoptosis of HT22 was detected by Annexin V/PI staining. (E) Western blot and (F) densitometry analysis of Cyclin D1, Bax and Bcl-2. Data were presented as mean ± SEM. *$p < .05$, compared with NC group; # $p < .05$, compared with LPS group.

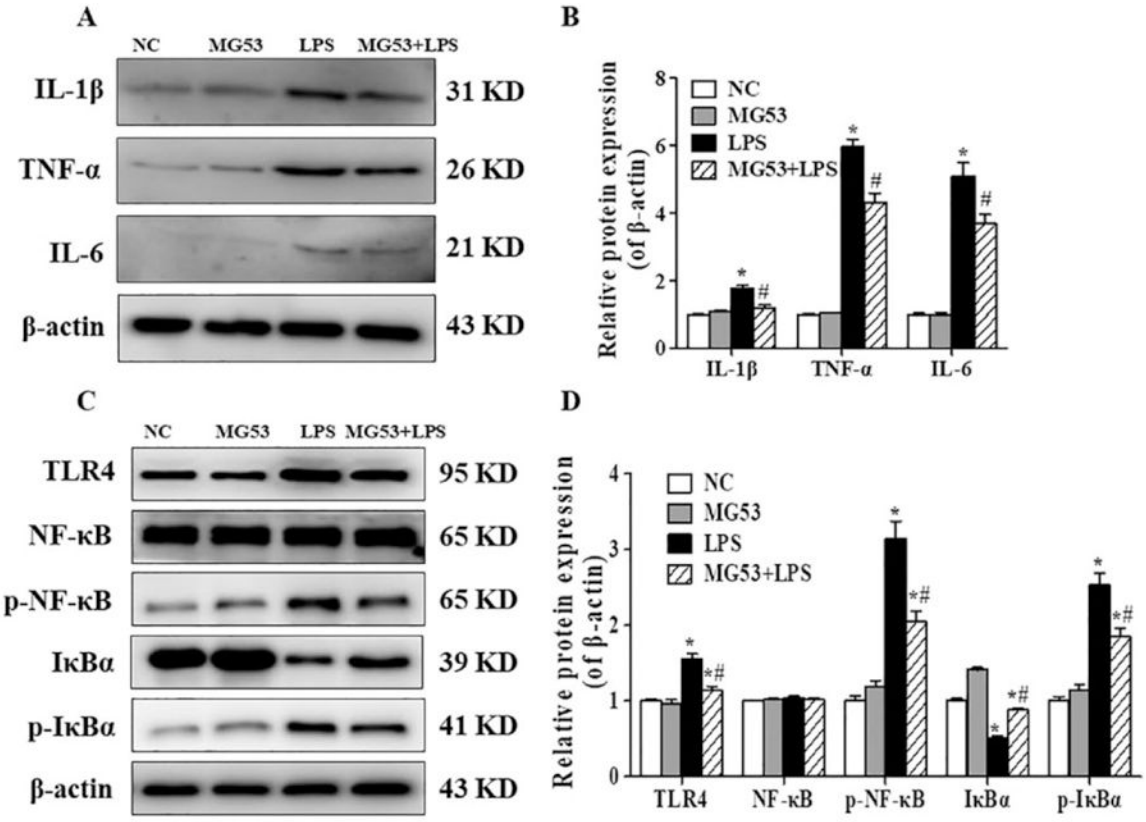

Fig. 3.

Effect of MG53 on LPS-induced proinflammatory cytokines expression and TLR4/NF-κB signaling proteins in LPS-treated HT22 cells. (A) Representative immunoblors and (B) densitometric analysis of IL-lβ, TNF-α and IL-6. (C) Representative immunoblots and (D) densitometric analysis of TLR4, total NF-κB, p-NF-κB, IKBα and p-IKBα. β-actin was used as an internal control. Data were presented as mean ± SEM. *$p < .05$, compared with NC group; # $p < .05$, compared with LPS group.

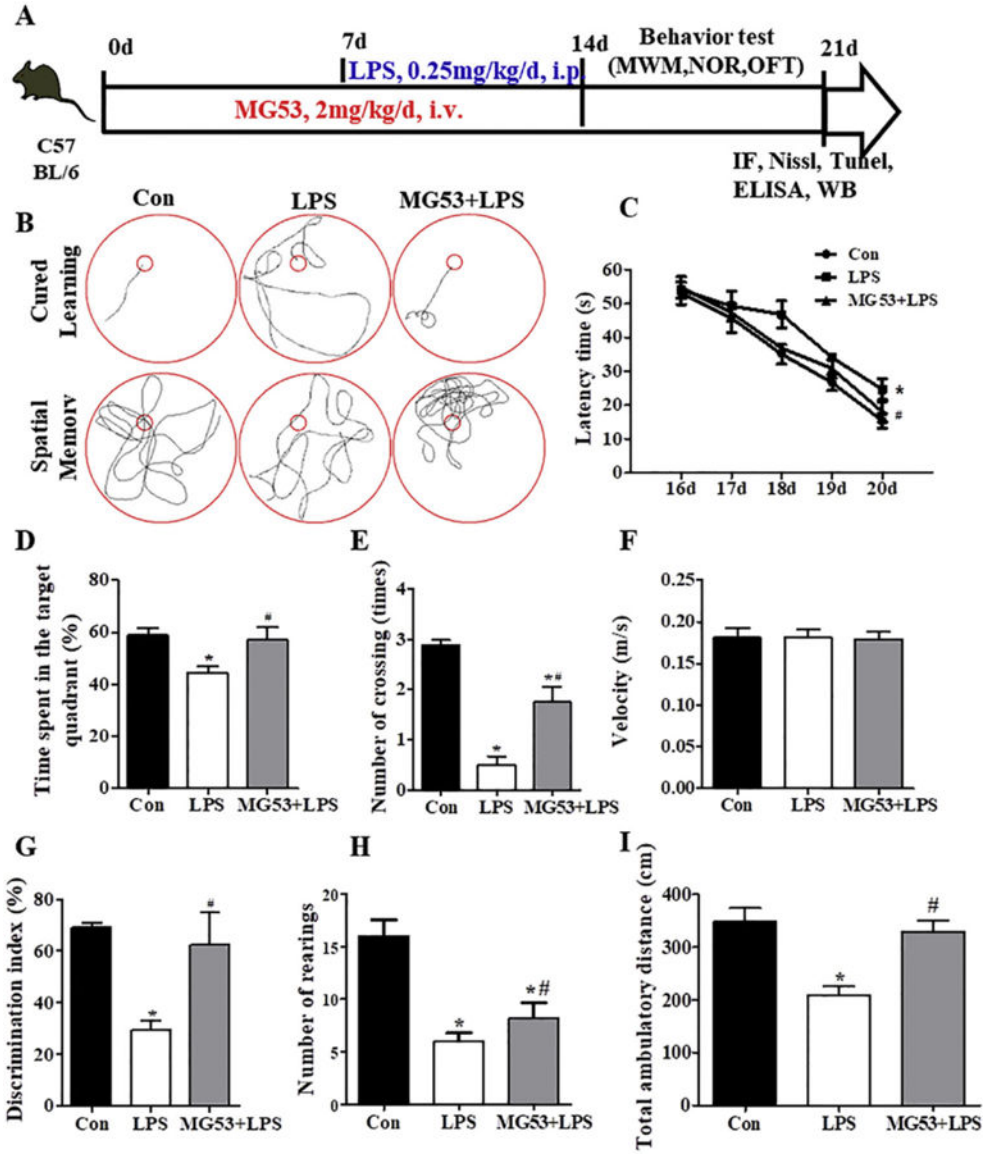

Fig. 4.

Effect of MG53 on LPS-induced memory impairment. (A) Schematic experimental protocol and timeline for experiment. (B) Representative swimming path from the MWM test. Escape latency (C), percentage of time spent in the target quadrant (D), crossing numbers (E) and swimming velocity (F) were measured and recorded in MWM test. (G) The discrimination index in the NOR test. (H) Total number of rearings and (I) total ambulatory distance in the OFT. Data were presented as mean ± SEM. $n = 6$ per group. *$p < .05$, compared with Con group; # $p < .05$, compared with LPS group.

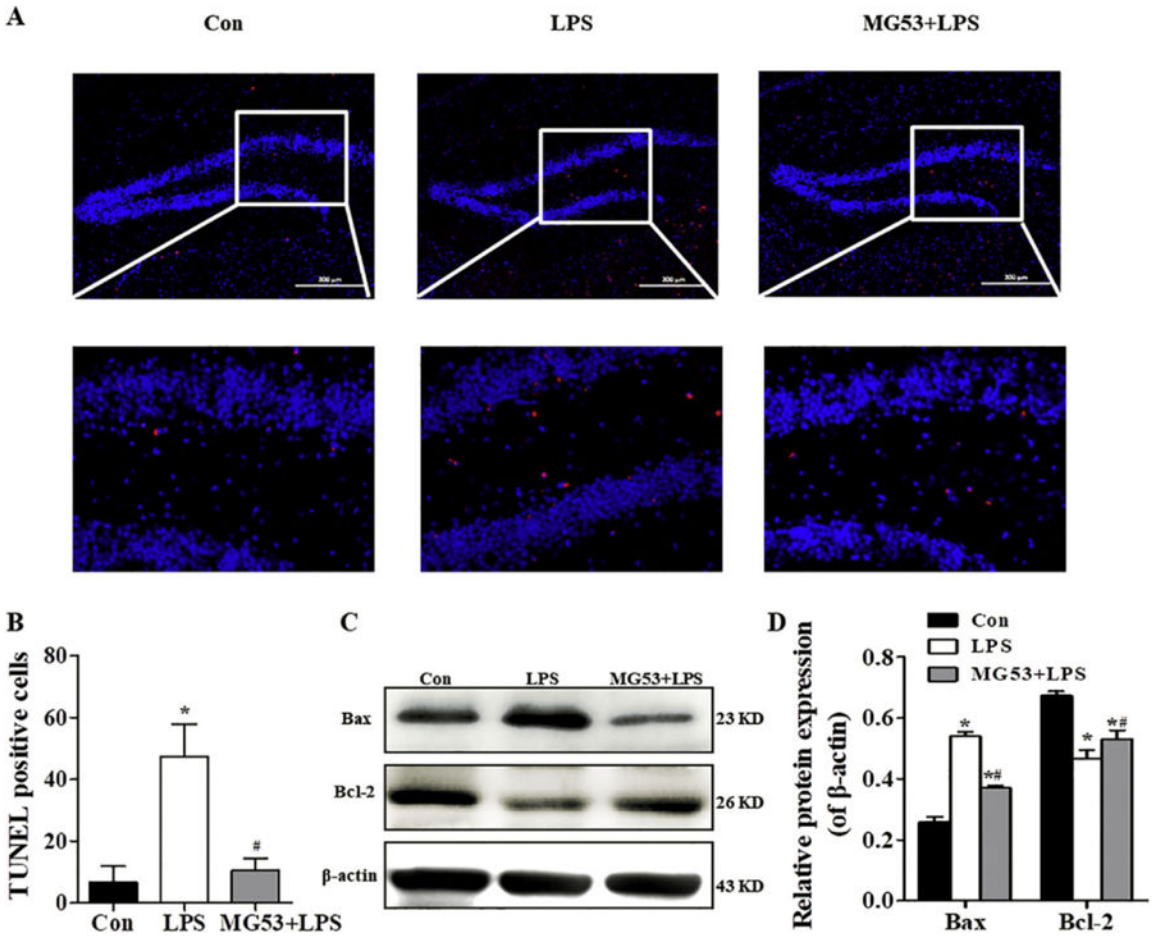

Fig. 5.

Effect of MG53 on neuronal cell death in LPS-treated mice. (A) Representative apoptotic neurons (red) in the hippocampus detected by TUNEL staining, Scale bar = 200 μm. (B) Quantitative analysis of TUNEL positive cells. (C) Representative immunoblots and (D) densitometric analysis of Bax and Bcl-2 in the hippocampus. β-actin was used as an internalcontrol. Data were presented as mean ± SEM. n = 6 per group. *$p < .05$, compared with Con group; # $p < .05$, compared with LPS group. (For interpretation of the references to colour in this figure legend, the reader is referred to the web version of this article.)

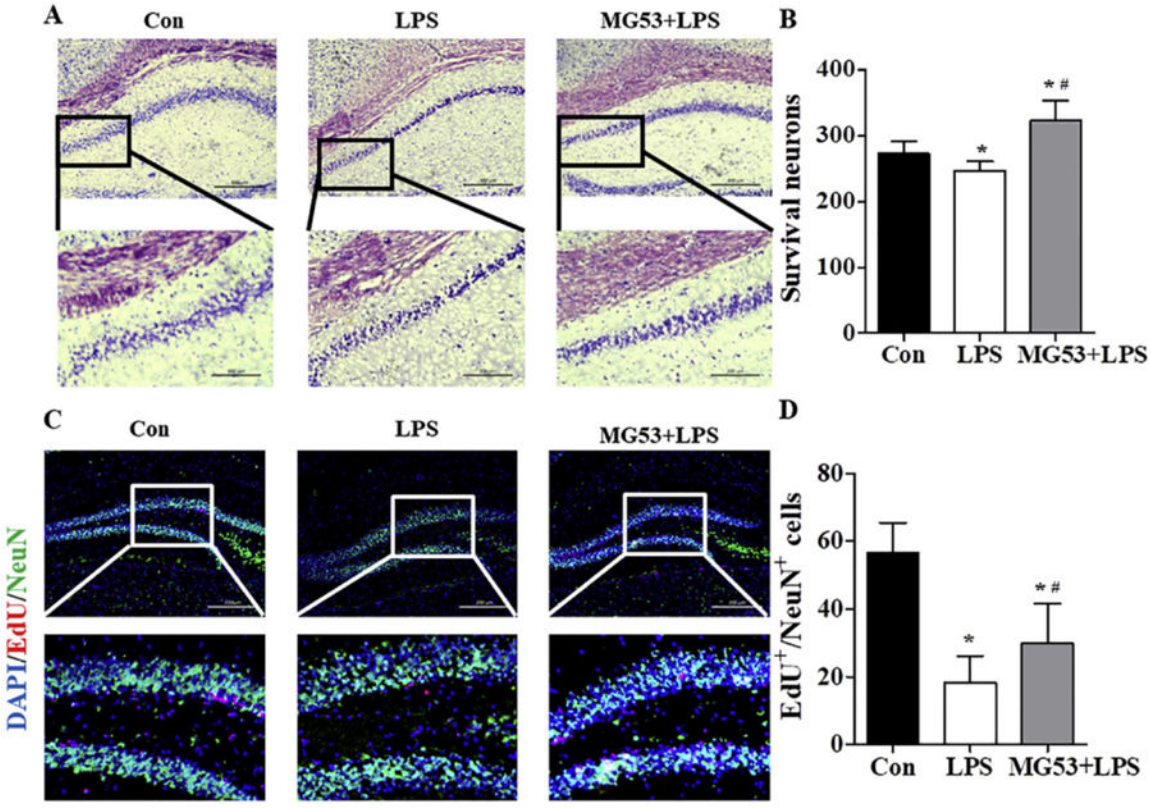

Fig. 6.

Effect of MG53 on neuronal survival and neurogenesis in LPS-treated mice. (A) Nissl staining of neurons in hippocampus. Scale bar (above) =200 μm, and scale bar (below) = 100 μm. (B) Quantitative analysis of Nissl bodies. (C) Representative immunofluorescent images and (D) quantification analysis of EdU/NeuN double staining in the hippocampus. Scale bar = 200 μm. β-actin was used as an internal control. Data were presented as mean ± SEM. $n = 6$ per group. *$p < .05$, compared with Con group; # $p < .05$, compared with LPS group.

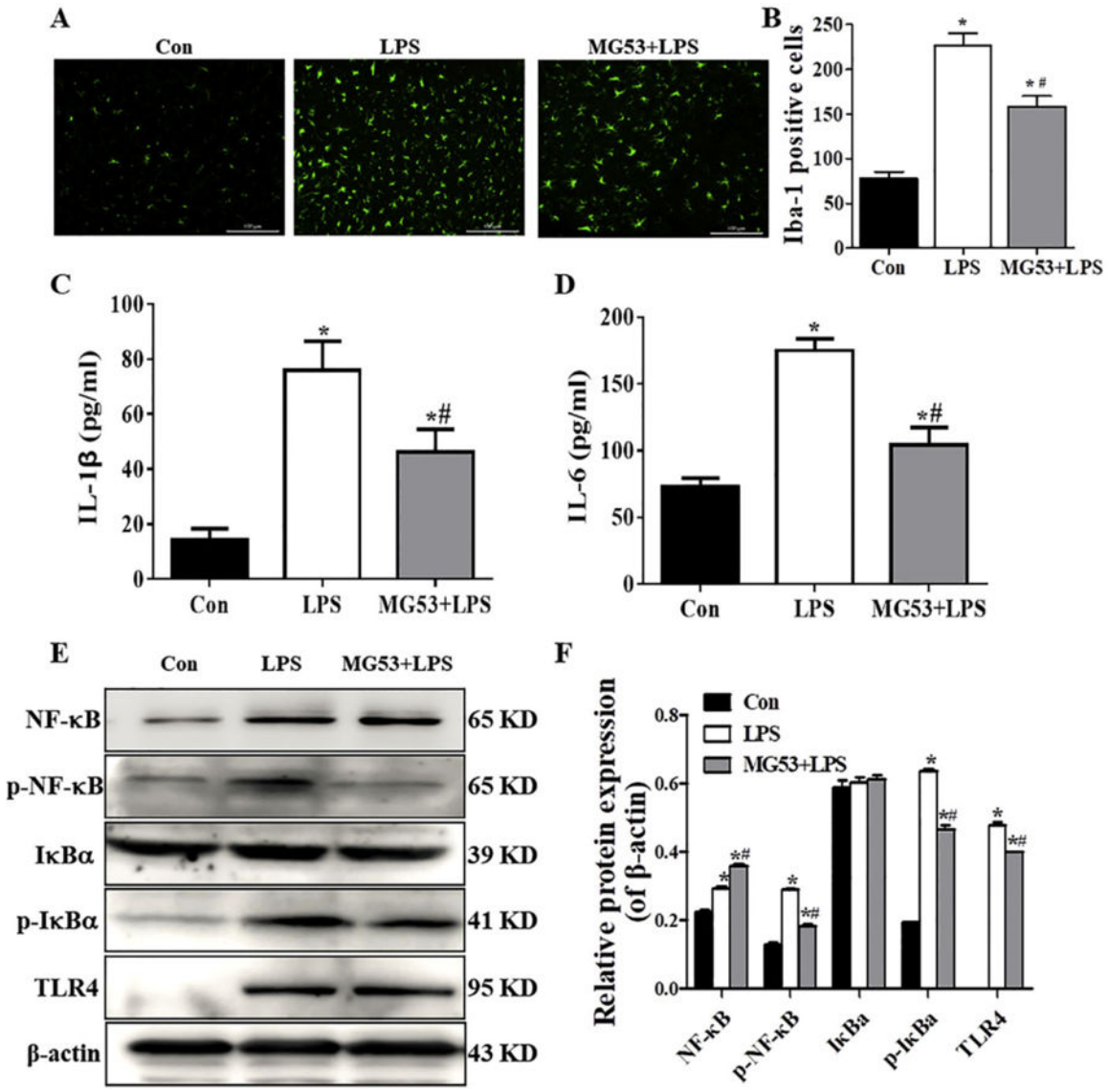

Fig. 7.

Effect of MG53 on microglia activation, inflammatory response and TLR4/NF-κB signaling protein expressions in LPS-treated mice. (A) Representative images of Iba-1 positive cells in the hippocampus. Scale bar = 100 μm (B) Quantification of the Iba-1 positive cells. Release of IL-1β (C) and IL-6 (D) was detected by ELISA. (E) Representative immunoblors and (F) densitometric analysis of TLR4, p-IκBα and p-NF-κB. β-actin was used as an internal control. Data were presented as mean ± SEM. $n = 6$ per group. *$p < .05$, compared with Con group; # $p < .05$, compared with LPS group.

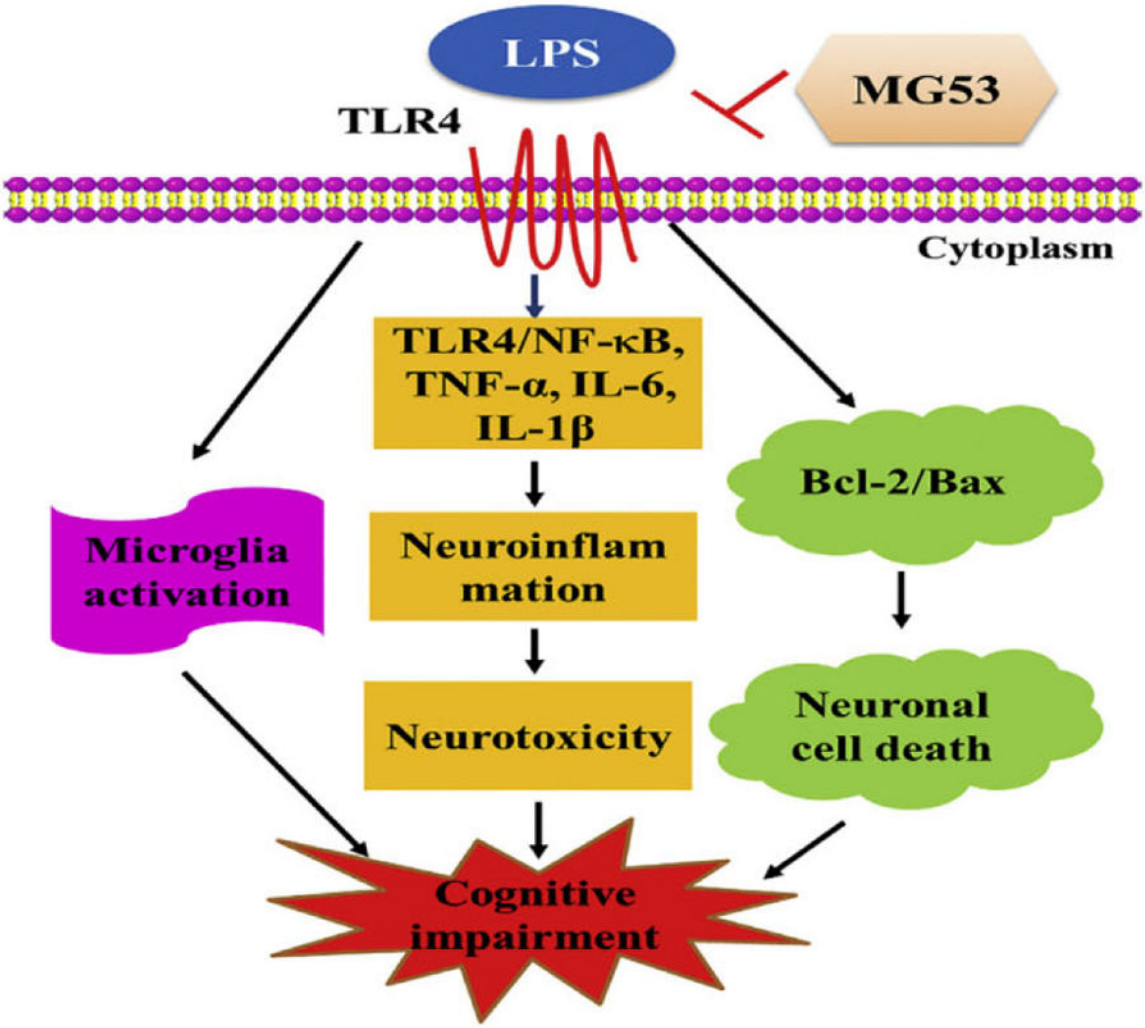

Fig. 8.
The possible mechanism of MG53 against LPS-induced neurotoxicity and neuroinflammation.